Research Article

Chemical Review and Letters
journal homepage: www.chemrevlett.com
ISSN (online): 2645-4947 (print) 2676-7279

Highly sensitive determination of nimesulide using glassy carbon electrode enhanced graphene oxide-multi-walled carbon nanotubes

Adil Abdulzahra Rashak[1, *], Faiq F. Karam[2]

[1]*Education Ministry, Education Directorate in Maysan, Maysan, Iraq*
[2]*Chemistry Department, Science Faculty, University of AL-Qadisiyah, Diwaniyah, Iraq*

ARTICLE INFO

Article history:
Received 24 July 2024
Received in revised form 12 August 2024
Accepted 23 August 2024
Available online 28 August 2024

eywords:
Nimesulide,
GO-MWCNTs,
Glassy Carbon Electrode,
CV, DPV.

ABSTRACT

Nimesulide (NIM) was determined utilizing (GO-MWCNTs/GCE) using differential pulse voltammetry (DPV). The impact of different experimental factors, such as scan rate, pH, and aggregation time, on the voltammetric responses of NIM was assessed. NIM achieved an irreversible electrochemical reaction controlled by the diffusion-controlled electrode method at GO-MWCNTS/GCE. This research examined the relationship between peak oxidation current and concentration under optimal conditions. A calibration curve was plotted showing the linear range of 0.06-0.8 ppm and limited of detection of 0.000318 ppm. The approach was effectively used to detect NIM in drugs as well as in human serum and urine samples. Results refer that the chosen method is fast, responsive, and cost-effective. The sensor (GO-MWCNTs/GCE) had an excellent reproducibility and good repeatability.

1. Introduction

Nimesulide (NIM) is an anti-inflammatory drug, which functions by stopping the prostaglandin production and by this means mitigating the pain caused. NIM too has antipyretic and analgesic assets, which utilized in the treatment of rheumatoid arthritis, osteoarthritis [1, 2]. However, excessive use of NIM causes severe side effects, both gastrointestinal (heartburn, abdominal discomfort, nausea, abdominal cramps, and diarrhea), and central nervous system (drowsiness, headache, dizziness), There are things that affect the genitourinary system (blood in the urine, decreased urination, and drowsiness) [3].

Nimesulide is a drug that is N-(4-nitro-2-henoxyphenyl) methane sulfonamide shown in Scheme 1. It is considered a non-steroidal anti-inflammatory drug (NSAID) and is non-acidic (pKa = 6.5) with administration as an antipyretic and analgesic. It inhibits Cyclooxygenase enzymes such as prostaglandin, which leads to a decrease in the production of prostaglandins. The strength of inhibition is moderate for cyclooxygenase 2 (COX-2), so the possibility of stomach injury and intolerance to the drug is less, and it is effective in reducing pain and inflammation Rheumatoid arthritis associated with osteoarthritis, it is also considered an anti-free radical, and helps protect tissue damage that may occur during inflammation[4].

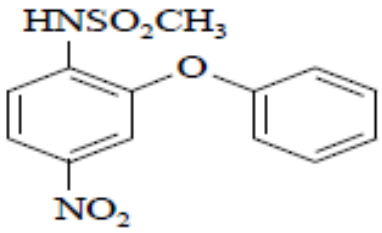

Scheme 1. Chemical structure of Nimesulide.

Expensive and tedious chromatographic techniques have been adopted to detect NIM [5-8] such as spectroscopic analysis. In comparison with other techniques, the electrochemical method exhibits high precision and less time consuming for bioactive molecules estimation [9-12]. In electrochemical methods, many bare electrodes are used with a modifier on their surface to estimate drugs [13-18]. However, few techniques are available for the estimation of NIM [19-22].

∗ Corresponding author; e-mail: adilsadi199011@gmail.com
https://doi.org/10.22034/crl.2024.469494.1390

Determination of NIM utilizing thin layer chromatography, high-performance liquid chromatography with UV technology, capillary zone electrophoresis, and spectrophotometry [23-27].

These methods are highly appreciated in analysis field, while they have drawbacks that make them undesirable in some analyzes or the search for an alternative to them. For example, it is not a routine analysis regarding those that require repeated analysis. The reason for this is due to equipment high cost, the need for an expert to operate it, and to test it for a long time, which is necessary. To overcome this problem, other methods have been developed, like electrochemical techniques which depends on electrodes. The approaches are more accurate and at ease in drug detection due to their short reaction time and rapid response. Cyclic voltammetry (CV), differential pulse voltammetry (DPV), square wave voltammetry (SWV), and many other voltammetric techniques and sensors have been employed in electrochemical drug detection approaches [28-30]. In latest years, electrodes have been developed to make their surfaces sensitive and have a larger surface area by adding non-toxic, chemically active materials that are less expensive and have ion exchange, diffusion or adsorption properties than are more porous [31-33]. Also, to improve the possibility of increasing the reading of the electric current curve, the surfaces of the electrodes can be modified using new carbon nanomaterials [34,35] with high surface area and high porosity, such as graphite oxide and carbon nanotubes. This permits the electrodes to sense the direction of the drugs to be administered more effectively [36-38].

To our knowledge, there are few electrochemical studies using a modified glassy carbon electrode in the determination of the drug NIM. Therefore, we sought to develop a method in this study, by enhancing (modifying) the surface of the glassy carbon electrode with a mixture of multi-walled carbon nanotubes (MWCNTs) and graphene oxide (GO). These modifications were synthesized and branded utilizing CV and DPV techniques for nimesulide quantification.

2. Computational details

Reagents and solutions

Pure Nimesulide (NIM) from xian veda chemical Co., Ltd., (98%) sulfuric acid H_2SO_4, $nitric\ acid\ HNO_3$ and (37%) HCl from B.D.H., from Fluka, (97.0%) NaOH From Sigma–Aldrich, (99%) KCl, (99.50%) Al_2O_3, acetic acid CH3COOH (glacial) (99.7%) and (99.5%) potassium hexacyanoferrate. From Merck, (99%) acetic acid, sodium acetate (99%), (85%) orthophosphoric acid, and (99.9%) boric acid. From Riedel-de-Haen, (99%) sodium phosphate dibasic heptahydrate and (98%). From Scharlau, absolute ethanol (99.99%) and sodium phosphate monobasic monohydrate. Buffer Solutions Preparation: 0.1M Acetate Buffer Solutions (ABS), 0.1M sulfuric acid, Phosphate Buffer Solutions (PBS), and0.1M Britton- Robinson Buffer Solutions (BR-BS), in this study, sulfuric acid is the best buffer solutions. Tab. labeled Nimesulide (NIM) 5 mg from citric labs Co., India.

Instruments and electrodes

Voltammetric measurements were conducted using the CH INSTRUMENTS CH660E (USA) with software HP PC. Electrochemical Glass Cell with a volume of 10mL involves 3 electrodes: (GCE) Glassy Carbon Electrode with 2 mm diameter, a Pt wire electrode serving as the counter electrode, and an (Ag/AgCl) Electrode with 3.0 M potassium chloride as the reference electrode. The experiment was conducted using CH INSTRUMENTS (USA).

Preparation of GO-MWCNTs/GCE

To obtain the cleaned surface electrode, the GCE firstly polished utilizing 0.05μm alumina-slurry on a polishing pad while until a clean mirror- surface achieved, subsequent to washing with distilled water. The GCE surface was cleaned by ultra-sonication in a solution of Milli-Q water and ethanol (1:1, v: v) for 5 minutes to remove any adsorbed contaminants. 0.1 grams of multi-walled carbon nanotubes were distributed in a 1.0 milliliter solution of (DMF) and sonicated for 2 hours. 15 microliters of multi-walled carbon nanotubes suspension which applied over the cleaned glassy carbon electrode surface and allowed to dry at ambient temperature.

Measurements of Voltammetric

The numbers of buffer solution were analyzed are four: 0.1M PBS, 0.1M APS, 0.1M BR-PS, and 0.1M H_2SO_4. The most effective one produced an oxidation peak for 0.0002M KET drug at 0.1M H_2SO_4. Three voltammetric techniques (CV, DPV, and SWV) were examined. The CV approach showed the most prominent oxidation peak (0.0002MNIM drug) in the existence of GO-MWCNTs/GCE, followed by the CV, SWV and DPV approaches. CV was conducted by assessing the potential within the limit of 0.4 to 1.6 V using a scan rate of 70 mV s^{-1} in a 0.1 M H_2SO_4 supporting electrolyte solution.

Calibration Curve

Measured solution was diluted to concentrations ranging from 0.06ppm to 0.18 ppm. A calibration curve was then constructed by plotting current versus concentration to determine the LOD, LOQ, and calibration graph.

Preparation of the commercial NIM drug

Pharmaceutical formulations containing (0.8, 1.0, 1.2) ppm of NIM from citric labs Co., India, were obtained from a local pharmacy. The tablet contains the next excipients as mentioned on the drug's leaflet: sucrose, tartaric acid, glucose, starch, magnesium citrate, lactose, and sodium bicarbonate.

The stock solution of the tablet sample was obtained by properly weighing and grinding one 100 mg NIM tablet in a mortar. The powder was stirred for 15 minutes in deionized water until completely dissolved. The mixture is filtered and then poured into a 0.5 L volumetric flask. Residual volume packed with a 0.04 M H_2SO_4 of supporting electrolyte solution. The current of the NIM tablet solution was measured and then from plotting the calibration curve the concentration of the tablets was estimated**.**

Samples Collecting

Urine samples were obtained from three species: healthy, non-smoking volunteers: V1 (30 years old, female), V2 (32 years old, male), and V3 (42 years old, male). For the real samples preparation, real urine samples of human were obtained Of individuals were in good health, and then diluted with 100 ml with electrolyte supporting before determining the concentration in urine and blood plasma. 1 mL of urine was added to the electrochemical cell and then filled up to 10 mL with supporting electrolyte. Later, the solution was appropriately mixed with a standard solution of NIM to get the desired concentration. The samples were analyzed for NIM utilizing the standard addition method with concentrations of 0.2 ppm, 0.4 ppm, and 0.6 ppm (n = 5).

1.0 ml of serum has been positioned in a centrifuge tube. A portion of the NIM stock solution was added to get the desired finishing concentration. The sample was thoroughly mixed utilizing a vortex mixer and subsequently centrifuged. The material from the centrifugation tube was moved into the voltammetric cell, and voltammograms were obtained for NIM by employing the addition method with concentrations of 0.3, 0.5, and 0.7 ppm (n= 5).

The statistical analysis having done, given the values for Recovery%, accuracy, Relative Standard Deviation (RSD), and Standard Deviation (SD).

3. Results and Discussion

Study of the best buffer solutions

Fig.1 shows the results of a cyclic voltammetry (CV) study on buffer solutions including 0.1M H_2SO_4, BRBS, ABS, and PBS. The study was conducted using a scan rate of 70 mV s^{-1} and a voltage range of -2.0 to 2.0 V, and it was conducted with a 2×10^{-4} M KET drug using bare GCE. The results showed a distinct oxidation peak in the buffer solution, which contained 0.1M H_2SO_4. Since buffer solutions of 0.1M (BR-PS, ABS, and PBS) did not show any oxidation peak, the NIM drug can be examined in the range of 0.1M H_2SO_4. However, a well-defined voltammetric profile and the largest magnitude and repeatability for the NIM oxidations signal were achieved with the 0.1M H_2SO_4 buffer solution, which was also the best overall result. When exposed to an electrode with a positive potential, the electroactive chemical NIM can move electrons from the solution to the electrode.

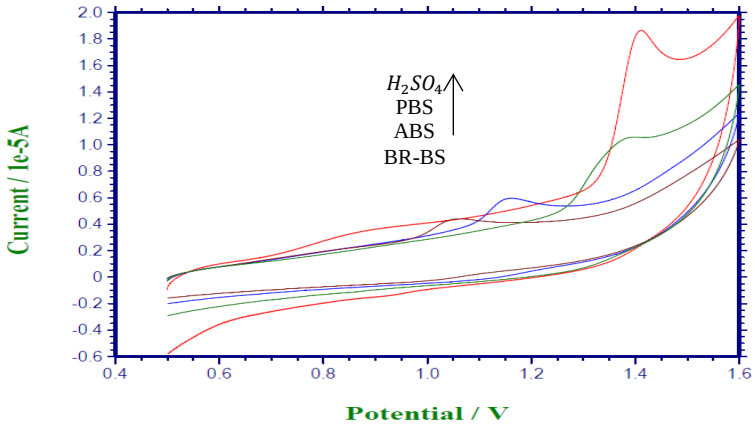

Fig. 1. Cyclic voltammograms (70 mVs^{-1}) in 0.1M (H_2SO_4, BRBS, ABS, and PBS) in the presence $2 \times 10^{-4} M\ NIM$.

Electrode modification by GO, MWCNTs and GO-MWCNTs/GCE

The study focused on enhancing the activity of the electrode surface via the incorporation of MWCNTs and GO. MWCNTs and GO were prepared separately and then mixed in equal amounts of 5 µmol each. The mixing caused an increase in the oxidation peak current of NIM compared to GO, MWCNTs, and the surface of the bare glassy carbon electrodes. Therefore, As a result, GO-MWCNTs/GCE was chosen for this study as Figure 2.

Surface Area

The determination of active surface of bare GE and GO-MWCNTs/GE was done using $5.00\,mM$ $K_3[Fe(CN)_6]$ in $0.10\,M$ of electrolyte (KCl) and CV were recorded by varying the scan rates utilizing the CV as publicized in [Figures (3) A, C]. By used the Randle–Sevcik eqn. 1, is useful for the surface area estimation of the working [38,39]:

$$ip\ a = (2.69 \times 10^5) n^{3/2} A\, Do^{1/2} C\ \mu^{1/2}) \quad (1)$$

Where ip the peak current of anode, n(n=1 reversible reaction) the electrons number, Do ($7.6 \times 10 - 6\ cms^{-1}$) the coefficient of diffusion, A the active surface area of the electrode, μ scan rate and C the concentration. Utilizing the slope of the plot $ip\ a$ *vs* $\mu^{\frac{1}{2}}$ (Fig. 3B, D),

$for\ bare\ GE: ip = 2.73784 \times 10^{-5}\mu^{1/2} + 7.08471 \times 10^{-5}$, $\boldsymbol{A = 0.06 cm^2}$

$for\ GO - MWCNTs/GE: ip = 7.1428 \times 10^{-4}\ \mu^{1/2} + 4.28339 \times 10^{-5}$, $\boldsymbol{A = 0.19\ cm^2}$

These results indicate that the surface area is larger than the geometric area ($0.031\ cm^2$) due to the effective surface area being significantly affected by the surface porosity GO-MWCNTs/GE [40].

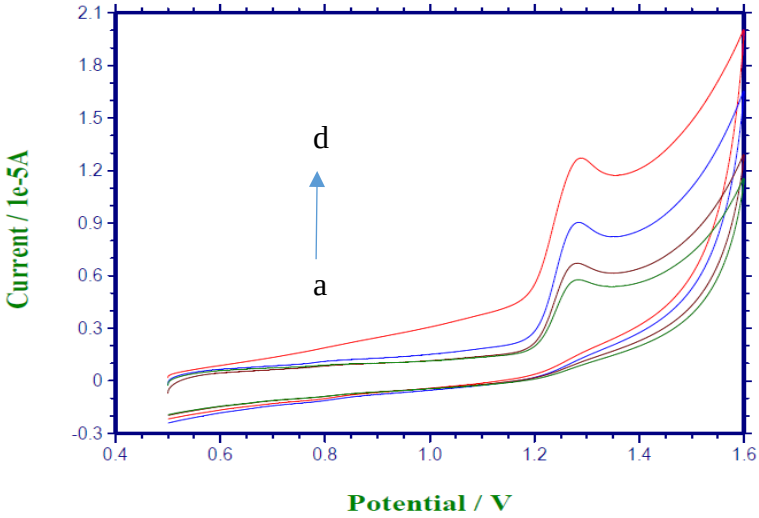

Fig. 2. Cyclic voltammograms (CV) $2 \times 10^{-4} M\ NIM$ at different modifications: (a) bare GCE (b) MWCNTs/GCE (c)GO/GCE and (d) GO+MWCNTs/GCE, at scan rate of 70 $mVs^{-1} in$ $0.04M\ H2SO4$

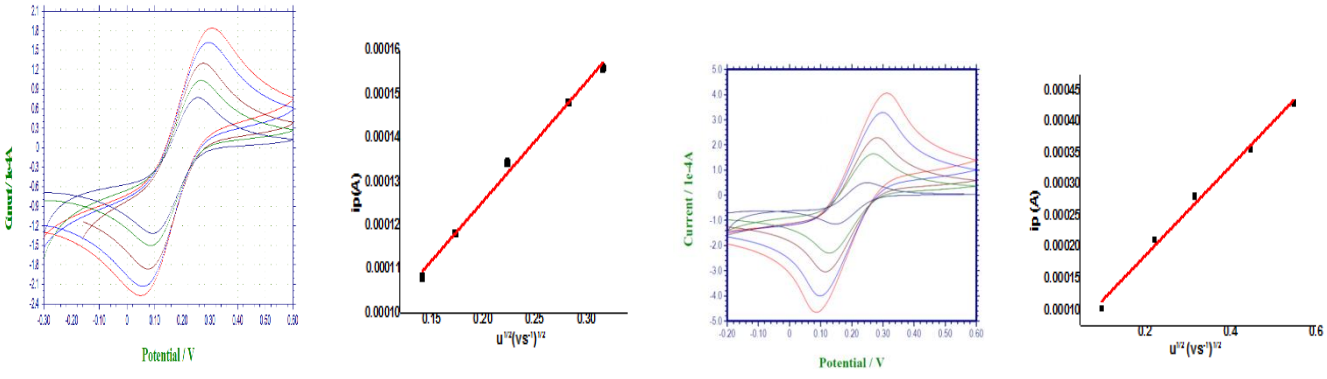

A B C D

Fig. 3. CV (A): bare GE and (C): GO-MWCNTs/GE. Plot of $ip\ a$ *vs* $\mu^{1/2}$at (B): bare GE and (D): GO-MWCNTs/GE.

Effect of pH

The impact of pH on a 2×10^{-4}M NIM medication was investigated using a scan rate of 70 mV s^{-1} across a pH range from 0.7-1.4. The influence of solution acidity on NIM was investigated by utilizing a $0.04M\ H_2SO_4$. The resulting voltammograms can be shown in Fig. 4A. An increase in pH of the electrolyte caused the peak of oxidation potential (Ep) to move into a more negative potential, suggesting the participation of a proton in the oxidation of NIM [41]. The electrochemical behavior of a 2×10^{-4}M solution of NIM is mostly influenced by the pH of the supporting electrolyte. The different voltammograms were acquired with changes in the oxidation potential and oxidation peak current [42–44]. Fig. 4A and 4B show that the NIM anodic peak current gradually increases as pH rises till reaching a pH of 1.1, then it decreases at pH 1.4 at ($0.04M\ H_2SO_4$) as a result of the protonation of the analyte. An observed shift in peak potential towards lower potential, accompanied by an increase in pH from 0.7 to 1.4, indicates proton involvement in the electrooxidation cycle. The peak current is influenced by the deprotonation and protonation state of the active species in the electrochemical cell. The current magnitude is directly related to the electrochemical reaction rate. NIM exhibits irreversible conduction at higher pH levels, such as pH 0.7–1.4. It is claimed that the oxidation of NIM is followed via an irreversible chemical reaction with hydrogen ions (H^+), particularly in acidic circumstances. The optimal sensitivity and form of the voltammogram are achieved at pH=1.1, resulting in the peak current of the analyte. Thus, a 0.04M H_2SO_4 solution with 1.1 pH of was selected as the best medium for voltammetric oxidations of NIM. Slope of the Ep versus pH graph was 0.0526 V/pH (Fig. 4C), $Ep = 1.40555 - 0.0526\ pH\ (r^2 = 0.9970)$. This result being near to the theoretical value of 0.05 suggests an equal number of electrons and protons present [45-47].

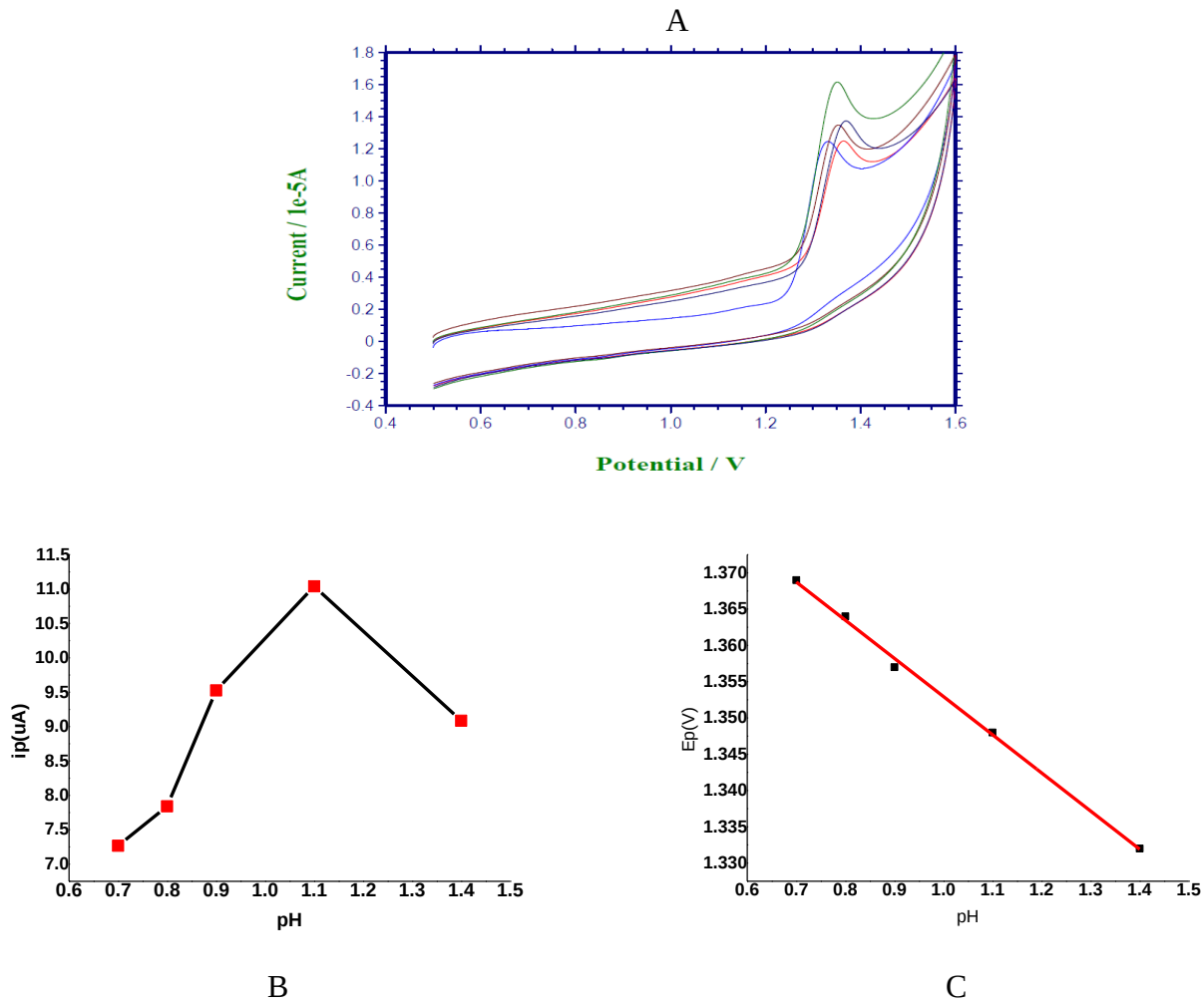

Fig. 4. (A) the effect pH= (0.7-1.4) for $\mathbf{2\times10^{-4}}\boldsymbol{M}$ NIM. (B) ip vs. pH. (C) Ep vs pH

Effect of scan rate

Valuable insights into electrochemical mechanisms may typically be obtained by examining the correlation between scan rate and peak current. Cyclic voltammetry was used to investigate the NIM voltammetric behavior across a range of scan rates, as shown in (Figure 5 A, B). Scan rate investigations were conducted to determine if the process on GO-MWCNTs/GCE was governed by diffusion or adsorption. The scanning was done within a range (20 - 100 mVs^{-1}) as in Figure 5C. A plot showing peak current (ip) against the square root of the scan rate ($\mu^{1/2}$) displayed a linear relationship with a correlation coefficient of 0.99723). The study focused on examining the characteristic of the limiting current by cyclic voltammetry (CV) technique. The peak current graph displayed a linear relationship, indicating that the oxidation peak current of NIM was governed by a controlled diffusion process [48]. This relationship can be mathematically stated as:

$$i_p = -30208 + 1.01289\,\mu^{\frac{1}{2}}, (r^2 = 0.99723)$$

Plot illustrating the logarithm of peak current of anode against the logarithm of scan rate resulted in a linear relationship with a slope of 0.91249 (Figure. 5D). The value closely aligns with the expected theoretical slope of 0.5 for a process solely controlled by diffusion [49-51], providing further evidence that the method is diffusion-controlled. This indicates that the electroactive NIM species transfers from the solution's bulk to an electrode's flat surface by diffusion. The data analysis resulted in the equation:

$$log i_p = -0.95777 + 0.91249\,log\mu\,, (r^2 = 0.99924)$$

Voltammetric studies were conducted at different scan rates to determine NIM under the best conditions, increasing the scan rate gradually from 20 to 100 mVs^{-1} , at a constant concentration of NIM results in an increase in background signal and a movement of the peak potential for a more negative value. This proves that oxidation of NIM is an irreversible process [52]. The S/N ratio was highest when the scan rate was set to 100 mVs^{-1}. The rate of 70 mVs^{-1} was selected for its ability to produce a distinct and well-defined peak current.

From the plot of E_p *vs* logμ (Fig. 5A and E), values of slope were estimated to equal 0.061 for oxidation peak. The close-fitting equations correlated with these data are $E_p = 1.241 + 0.061\,\log\mu$ ($r^2 = 0.99925$). The slope of the plot was utilized to estimate the value of αn and electrons number of reaction. For irreversible process, the Laviron's equation (2) could be written as [53]:

$$E_p = E_o + [2.303RT / \alpha nF]log[RT\,K_s / \alpha nF] + [2.303RT / \alpha nF]log\,\mu \quad (2)$$

Where, E_o the official standard redox potential, α charge transfer coefficient, $K_s$the constant of rate, n the electrons contributed. For the irreversible electrode process the value of α = 0.5,$T = 298\,K, R = 8.314\,JK^{-1}mol^{-1}, and\ F = 96485\,Cmol^{-1}$, and (n value) for the anodic peak the was found ($slope = [2.303RT / \alpha nF]$) to 1.94 (≈2.0). Scheme 2 show the proposed mechanism detailed. Through Equation No. 2, it is possible to draw the curve between Ep and $log\,\mu$, and the extrapolation point on the vertical axis at μ = 0 can obtain E_o, and thus the value of Ks can be calculated. [54], E_o were1.125V, From the overhead, calculated K_s values were $3963/s$. The value of surface coverage (Γ) can be obtained from Equation No. (3) ; through the slope of the curve between ip versus μ (Fig. 5B) could be estimated from [$i_p = 0.3858 + 0.06979\,\mu(r^2 = 0.9970)$], the $slope = 0.0697\,\mu A(mV^{-1})^{-1}$ become 69.7 $\mu A(V^{-1})^{-1}$, $A = 0.19cm^2$, the value the Γ for GO-MWCNTS/GE equivalent to $97.76 \times 10^{-9}\,molcm^{-2}$(97.76 $nmolcm^{-2}$).

$$i_p = \left(\frac{n^2F^2}{4RT}\right)\Gamma\,A\,\mu \quad (3)$$

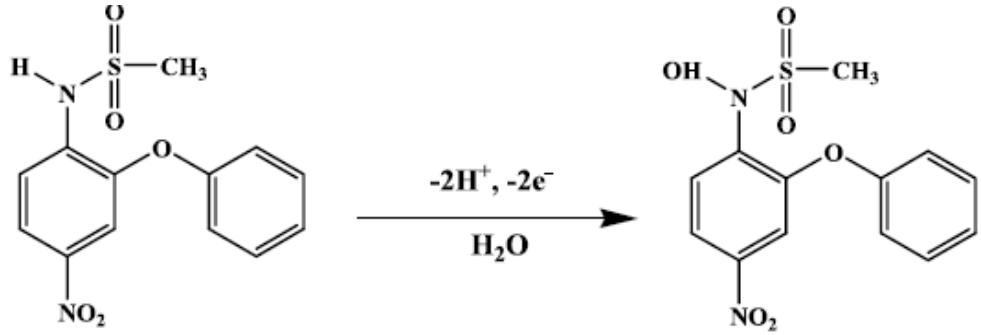

Scheme 2. Proposed mechanism for oxidation of NIM

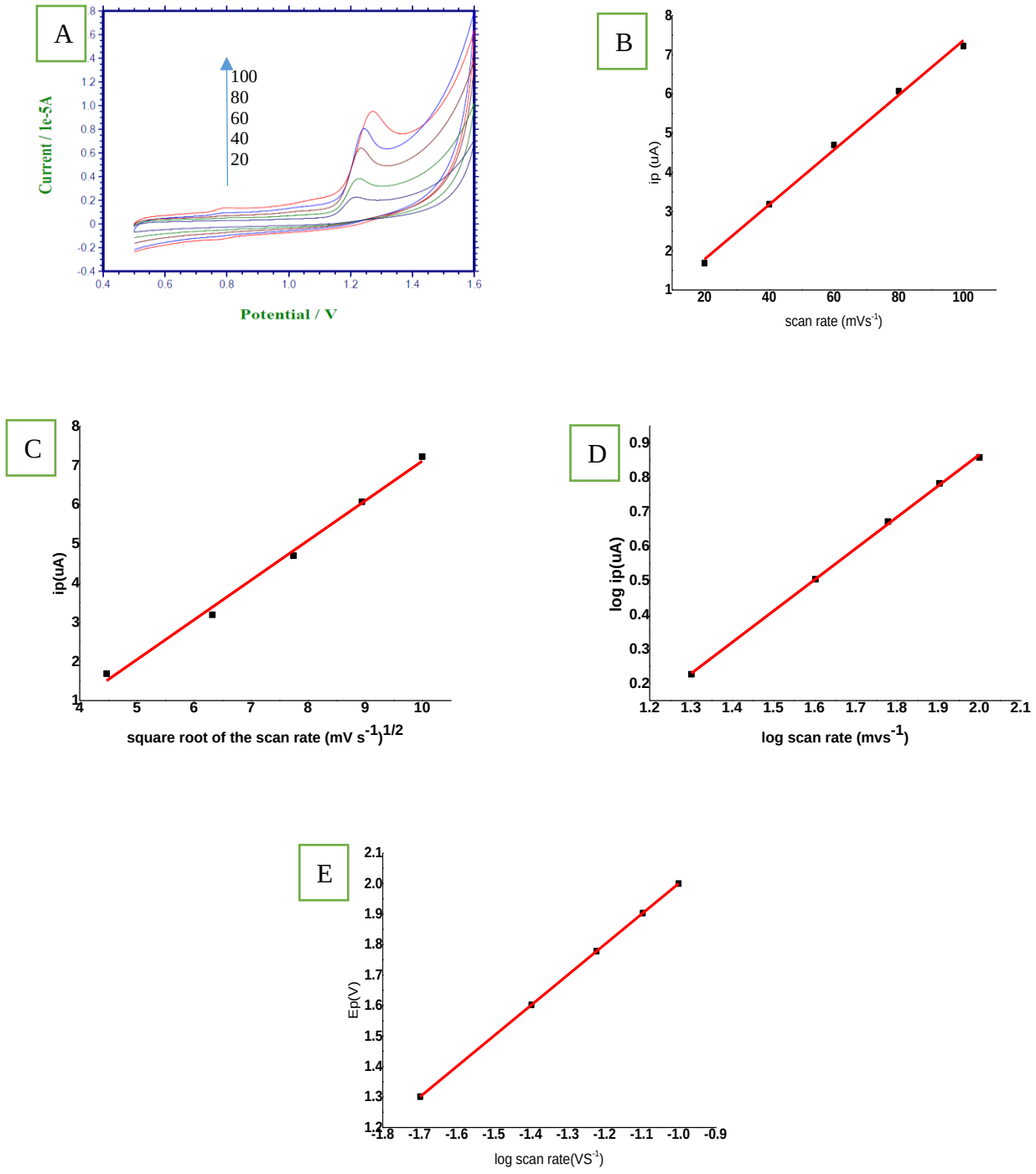

Fig. 5. (A) Voltammograms of GO-MWCNTs/GCE at different scan rates (B) plot of $i_p$vs μ (C) plot i_p vs of square root of scan rate (D) plot of log $i_p$vs log μ and (E) plot of E_p *vs log* μ

Effect of accumulation times

Open circuit potential (OCP) accumulation is a common technique in electroanalytical chemistry to aggregate analytes to increase sensitivity in determination. Fig. 6 shows the effect of accumulation time, ranging from 0 to 900 s, on the oxidation of NIM at GO-MWCNTs/GCE. The potential diminished progressively as the accumulation duration went from 0 to 600 seconds. With further increase, the peak potential stabilizes after an accumulation time of 600 seconds.

Hence, 600-second accumulation duration was used in subsequent studies. The peak current of NIM slightly varied with the variation in accumulation potential. The peak current through NIM was unaffected by the accumulating potential. Therefore, open-circuit conditions were employed for the accumulation.

Calibration curve

Fig. 7A displays the voltammograms of NIM for various concentrations using (DPV) between 0.06 to 0.18 ppm. The oxidation peak current rises as the NIM concentration increases, indicating a linear correlation between ip and NIM concentration. Results indicated a linear connection between the peak current (ip) and the conc. of NIM in the range of 0.06-0.18 ppm, as depicted in Fig. 7B. The equation is:

ip (uA) = 38.12 + 5.00 C (ppm) (r^2=0.99993).

The DPV analysis revealed a direct correlation between the oxidation peak current and the concentration of NIM, as the anodic peak current increases with the increase in NIM concentration. This outcome suggests that the procedure is suitable for estimating NIM in various samples.

The limit of detection (LOD) of an analytical method is the minimum amount of analyte in a sample that can be detected but not necessarily measured precisely. At S/N of 3 (LOD=3s/m), (n=8), the limit of detection for NIM was determined to be 0.000318 ppm using DPV under ideal conditions. The limit of quantitation (LOQ) is the minimum amount of analyte in a sample that can be accurately and precisely measured using a specific analytical method. LOQ for NIM with a (S/N) ratio of 10 (LOQ=10s/m) (n=8) determined to be 0.00106 ppm for DPV under optimal conditions.

The method proposed in the scope of this study gave a linear range with a detection limit equivalent to or lower (better) than that studied in the literature using chemically modified electrodes as shown in Table 1. Our method is efficient and rapid for quantifying NIM concentration, with LOD of 0.000318ppm, as indicated by the findings. The results indicate that DPV technology may be used to estimate NIM in samples due to its environmentally benign nature, time efficiency, and low detection limit.

Analytical applications

Pharmaceutical tablets analysis

100 mg of NIM tablets drug was dissolved in 1000 ml of the electrolyte solution to conduct a DPV analysis. The oxidation current of different concentration NIM (0.8, 1, 1.2) ppm, was measured and found to be equal to 42.15, 43.14, 44.13 uA. Through the calibration curve from standard solutions, using equation: ip(uA) = 38.12 + 5.00 C(ppm) (r^2= 0.99943).The concentration of the NIM was evaluated by ratio and proportional calculations, revealing a presence of (0.806, 1.004, 1.202) ppm of the drug as indicated in table 2. The results obtained for quantifying NIM closely align with the supplier's recommendations, with a recovery rate of 100.75%, 100.4%, 100.17%, demonstrating the effectiveness of the sensor for practical analysis.

Biological fluids assay application

The suggested method's applicability was assessed by estimating the recovery of NIM in human serum and urine samples. Prepared samples were analyzed utilizing the usual addition procedure. The data offered in table 3 indicates positive outcomes. The practical usefulness and reliability of the glassy carbon electrode surface modified with GO-MWCNTs in estimating NIM in biological samples such as serum and urine were measured. This supports the analysis of NIM in the samples (plasma and urine). No detectable NIM content was present in biological fluids. Therefore, a specific quantity of NIM was introduced into the human serum and urine samples. The NIM concentration was estimated using the DPV approach and calibration plot designed for biological fluids, ip (uA)=38.12+5.00C (ppm) (r^2=0.99993).The oxidation peak vs current was determined for each concentration of NIM in blood and urine samples from three healthy volunteers by conducting one test per subject. This data was used in the linear regression equation to calculate the NIM concentration.

Repeatability, reproducibility and stability

To evaluate the applicability of electrochemical sensors, the stability, reproducibility, and repeatability of a glass electrode modified with GO-MWCNTs were studied. By repeating the reading five times in a row, it was almost observed that the GO-MWCNTs sensor has a high repeatability in NIM estimation; RSD = 1.52% was obtained; this indicates that GO-MWCNTs have good repeatability.

Seven modified electrodes were made under the same experimental conditions to study the reproducibility of NIM estimation; It was noted that the reproducibility is excellent because RSD = 1.84%.

GO-MWCNTs/GCE sensor stability to 0.0002M NIM in 0.04M $H_2SO_4$was also observed periodically. After stored for 5 days at $4\,°C$ in a refrigerator, the

anodic current gotten from the as-prepared electrode continued practically similar. Also, under the same experimental conditions under study, for ten days the electrode was stored, the anodic peak current was stable and maintained about 98.75% of its original value, which represents the high stability possessed by GO-MWCNTS.

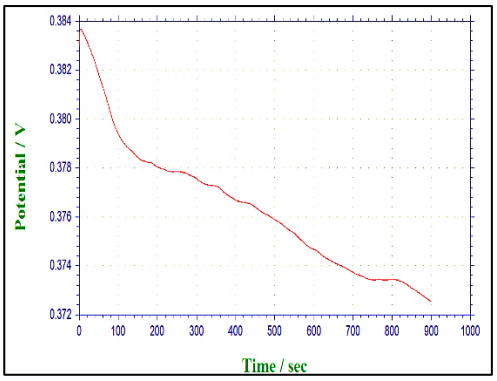

Fig. 6. Effect of accumulation time on the oxidation peak potential at $2 \times 10^{-4} M$ NIM in $0.04 M\ H_2SO$ for GO- MWCNTs/GCE.

Table 1. Literature results with this study to estimate the LOD for NIM.

LOD(ppm)	linear range (ppm)	Methods	Years	Reference
0.03	0.05-5	*HPLC*	1999	55
0.01	0.01-2	*HPLC*	2001	56
0.0154	0.0308-3.08	*DPV*	2006	57
0.05	0.01-1	LCM	2008	58
0.0493	0.1-20	LCV	2010	59
0.0400	0.81-31	DPV	2011	60
0.297	10—50	Amperometry	2013	61
0.001	0.0308–12.32	DPV	2016	62
0.001078	0.00308-462	Amperometry	2017	63
0.004928	0.1078-0.616	SWV	2018	64
0.000311	0.00308-0.1078	SWV	2020	65
0.04312	0.0095–0.539	ASP	2021	66
0.000310	0.06-0.18	DPV	2024	This work

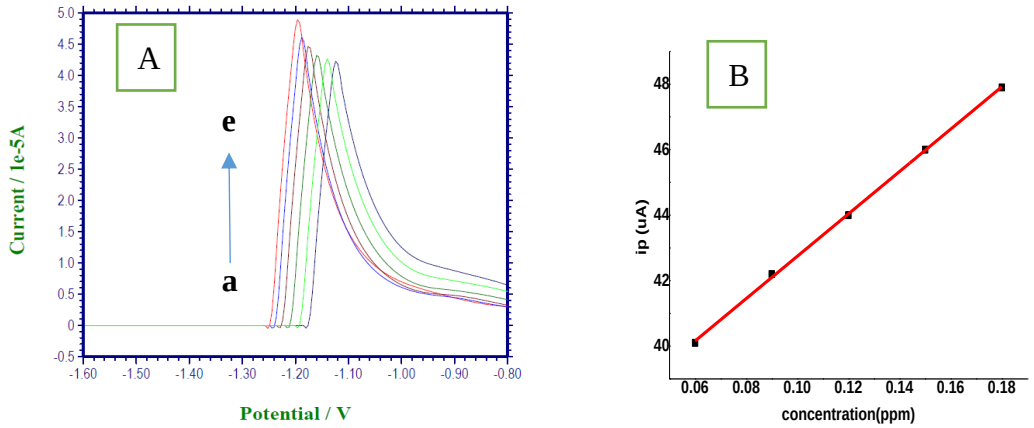

Fig. 7. (A) DPV for concentration of NIM (ppm): (a) 0.06 (b) 0.09 (c) 0.12 (d) 0.15(e) 0.18 (B) Plot of current vs. concentration of NIM.

Table 2. Determination of NIM in pharmaceutical tablet

Sample	Added (ppm)	Found (ppm)	Recovery%	S.D[a]	RSD[b]	Accuracy (bias%)
NIM	0.800	0.806	100.75	0.493	1.17	0.75
NIM	1	1.004	100.4	0.495	1.15	0.40
NIM	1.2	1.202	100.17	0.523	1.18	0.17

a= standard deviation, b= relative standard deviation.

Table 3. Determine of NIM in biological fluids

Sample	**Added NIM (ppm)**	**ip (*uA*)**	**Found NIM (ppm)**	**Recovery %**	**S.D**	**RSD**	**Accuracy (bias%)**
Urine	0.2	39.10	0.196	98.00	0.03	0.077	-0.4
	0.4	40.13	0.402	100.50	0.08	0.20	0.5
	0.6	41.11	0.598	99.67	0.04	0.10	-0.3
Serum	0.3	39.63	0.302	100.67	0.07	0.18	0.7
	0.5	40.61	0.498	99.60	0.09	0.22	-0.4
	0.7	41.64	0.704	100.57	0.07	0.17	0.57

4. Conclusion

This work explores the electrochemical oxidation of NIM utilizing the GO-MWCNTs/GC electrode by cyclic and differential pulse voltammetry with a sulfuric acid supporting electrolyte. Analysis of pH changes indicated the involvement of protons in the electro-oxidation process. The proposed mechanism detailed the involvement of two electrons and two protons in the oxidation process. Forward voltammograms displayed peaks, however no peaks were seen in the reverse scan, indicating an irreversible reaction of NIM. The investigation of the scan rate indicated that the process is regulated by diffusion approach and calculation the rate constant K_s and surface coverage. A linear range of 0.06-0.8 ppm was identified for MIM concentration, with LOD and LOQ values determined as 0.000318 ppm and 0.00106 ppm, respectively. The approach can be used to detect various drugs in biological samples such blood serum and urine. The GO-MWCNTs sensor for GC electrode surface modification has good repeatability and reproducibility. It is beneficial for generating real clinical data in clinical laboratories.

Acknowledgements

The authors express their gratitude to the Science College, University of AL-Qadisiyah, Diwaniyah, for their big provision and continues support.

References

[1] I. Chabri, Y. Benhouria, A. Oubelkacem, A. Kaiba, I. Essaoudi, A. Ainane, SCAPS device simulation study of formamidinium Tin-Based perovskite solar Cells: Investigating the influence of absorber parameters and transport layers on device performance, Solar Energy 262 (2023) 111846.
[1] R. Davis, R.N. Brogden, Drugs 48 (1994) 431–454.
[2] A. Bernareggi, Clin. Pharmacokinet. 34 (1998) 247–274.
[3] I. Bjarnason and B. Thjodleifsson, Rheumatology, 38 (1999) 24.
[4] Bernareggi A. Clinical pharmacokinetics and metabolism of nimesulide. Inflammopharmacology, 9 (2001) 81-89.
[5] A. Maltesh, F. Maugeri, C. Bucolo, J. Chromatogr. B 804 (2004) 441–443.
[6] C.K. Zacharis, P.D. Tzanavaras, M. Notou, A. Zotou, D.G. Themelis, J. Pharaceut. Biomed.Anal 49 (2009) 201–206.
[7] B. Hemmateenejad, K. Javidnia, M. Saeide - Boroujeni, J. Pharm. Biomed. Anal. 47 (2008) 625–630.
[8] I.C. Constantinescu, M. Florea, C.C. Arama, A. Nedelcu, C.M. Monciu, Farmacia 57 (2009) 267–271.
[9] N.P. Shetti, D.S. Nayak, S.J. Malode, R.M. Kulkarni, Sens. Actuators, B 247 (2017) 858–867.
[10] A. Khodadadi, E. Faghih-Mirzaei, H. Karimi-Maleh, A. Abbaspourrad, S. Agarwal, V.K. Gupta, Sens. Actuators B Chem. 284 (2019) 568–574.
[11] F. Tahernejad-Javazmi, M. Shabani-Nooshabadi, H. Karimi-Maleh, Compos. Part B 172 (2019) 666–670.
[12] H. Karimi-Maleh, C.T. Fakude, N. Mabuba, G.M. Peleyeju, O.A. Arotiba, J. Colloid Interface Sci. 554 (2019) 603–610.

[13] B. Avinash, C.R. Ravikumar, M.R.A. Kumar, H.P. Nagaswarupa, M.S. Santosh, A. S. Batt, D. Kuznetsov, J. Phys. Chem. Solids 134 (2019) 193–200.
[14] S. Felix, A.N. Grace, R. Jayavel, J. Phys. Chem. Solids 122 (2018) 255–260.
[15] A. Karthika, S. Selvarajan, P. Karuppasamy, A. Suganthi, M. Rajarajan, J. Phys. Chem. Solids 127 (2019) 11–18.
[16] L. Jothi, S. Neogi, S.K. Jaganathan, G. Nageswaran, Biosens. Bioelectron. 105 (2018) 236–242.
[17] S.D. Bukkitgar, N.P. Shetti, R.M. Kulkarni, M.R. Doddamani, J. Electroanal. Chem. 762 (2016) 37–42.
[18] R. Salahandish, A. Ghaffarinejad, S.M. Naghi, A. Niyazi, K. Majidzadeha, M. Janmaleki, A.S. Nezhad, Sci. Rep. 9 (2019) 1226.
[19] O.G. Makukha, L.A. Ivashchenko, O.A. Zaporozhets, V.O. Doroschuk, Chem. Pap. 73 (2019) 693–699.
[20] P.B. Deroco, R.C. Rocha-Filho, O.F. Filho, Talanta 179 (2018) 115–123.
[21] K.F.D. Pino, L.N. Oliveira, M.J. Silva, O. Caon-Filho, T.R.L. Dadamos, J. Appl. Spectrosc. 85 (2019) 1151–1157.
[22] S.D. Bukkitgar, N.P. Shetti, R.M. Kulkarni, S.B. Halbhavi, M. Wasim, M. Mylar, P. S. Durgi, S.S. Chirmure, J. Electroanal. Chem. 778 (2016) 103–109.
[23] V.B. Patravale, S. Souza, Y. Narkar, J. Pharm. Biomed. Anal. 25 (3–4) (2001) 685–688.
[24] D. Dogrukol-Ak, M. Tuncel, H.Y. Aboul-Enein, J. Sep. Sci. 24 (2001) 743–748.
[25] C.S.R. Lakshmi, M.N. Reddy, Mikrochim. Acta 132 (1999) 1–6.
[26] S. Chandran, S. Saggar, K.P. Priya, R.N. Saha, Drug Dev. Ind. Pharm. 26 (2000) 229–234.
[27] B. Miljkovic, B. Brzakovic, I. Kovacevic, D. Agbaba, M. Pokrajac, J. Plan. Chromatogr.-Modern TLC 16 (2003) 211–213.
[28] L. Svorc, D. M. Stankovic, E. Mehmeti, and K. Kalcher, Anal. Methods 6 (2014) 4853.
[29] L. Svorc, D. M. Stankovic, and K. Kalcher, Diam. Relat. Mater. 42 (2014) 1.
[30] D. M. Stankovic, L. Svorc, E. Mehmeti, and K. Kalcher, Microchem. J. 118 (2015) 95.
[31] Z. Navratilova, P. Kula, Clay modified electrodes: present applications and prospects, Electroanalysis 15 (2003) 837–846.
[32] C. Mousty, Biosensing applications of clay-modified electrodes: a review, Anal. Bioanal. Chem. 396 (2010) 315–325.
[33] S.M. Macha, A. Fitch, Clays as architectural units at modified electrodes, Mikrochim. Acta 128 (1998) 1–18.
[34] A. K. O. Aldulaim, N. M. Hameed, T. A. Hamza, A. S. Abed, The antibacterial characteristics of fluorescent carbon nanoparticles modified silicone denture soft liner. *J. Nanostruct.*, 12 (2022) 774-781.
[35] (a) A. Karbakhshzadeh, S. Majedi, V. Abbasi, Computational investigation on interaction between graphene nanostructure BC3 and Rimantadine drug: Possible sensing study of BC3 and its doped derivatives on Rimantadine, *J. Chem. Lett.* 3 (2022) 108-113. 10.22034/jchemlett.2022.352857.1079; (b) B. Ghanavati, A. Bozorgian, J. Ghanavati, Removal of Copper (II) Ions from the Effluent by Carbon Nanotubes Modified with Tetrahydrofuran, *Chem. Rev. Lett.* 6 (2022) 68-75. 10.22034/crl.2022.326950.1152; (c) B. Ajdari, S. A. Vahed, Fullerene (C20) as a sensing material for electrochemical detection of Nortriptyline: A theoretical study, *J. Chem. Lett.* 3 (2022) 164-168.10.22034/jchemlett.2023.385007.1104; (d) E. Vessally, M. R. Ilghami, M, Abbasian, Investigation the Capability of Doped Graphene Nanostructure in Magnesium and Barium Batteries with Quantum Calculations, Chem. Res. Technol., 1 (2024) 10.2234/chemrestec.2024.436837.1007.
[36] (a) N. Teradal, J. Seetharamappa, Bulk modification of carbon paste electrode with Bi2O3 nanoparticles and its application as an electrochemical sensor for selective sensing of anti-HIV drug nevirapine, Electroanalysis 27 (2015) 2007–2016; (b) N. Nesakumar, S. Sethuraman, U. Maheswari Krishnan, J.B. Balaguru Rayappan, Electrochemical acetyl choline sterase biosensor based on ZnO nanocuboids modified platinum electrode for the detection of carbosulfan in rice, Biosens. Bioelectron. 77 (2016) 1070–1077; (c) A.F. Shojaei, K. Tabatabaeiana, S. Shakeri, F. Karimi, A novel 5-fluorouracile anticancer drug sensor based on ZnFe2O4 magnetic nanoparticles ionic liquids carbon paste electrode, Sensors Actuators B Chem. 230 (2016) 607–614.
[37] N.S.K. Gowthaman, B. Sinduja, S. Abraham John, Tuning the composition of goldsilver bimetallic nanoparticles for the electrochemical reduction of hydrogen peroxide and nitrobenzene, RSC Adv. 6 (2016) 63433–63444.
[38] N.P. Shetti, S.J. Malode, S.T. Nandibewoor, Electro-oxidation of captopril at a gold electrode and its determination in pharmaceuticals and human fluids, Anal. Methods 20 (2015) 8673–8682.
[39] D. Ilager , H. Seo , N.P. Shetti , S.S. Kalanur , CTAB modified Fe-WO3 as an electro- chemical detector of amitrole by catalytic oxidation, J. Environ. Chem. Eng. 8 (6) (2020) 104580.
[40] Raeisi-Kheirabadi N.; Nezamzadeh-Ejhieh A.; Aghaei H. A brief study on the kinetic of the voltammetric behavior of the modified carbon paste electrode with NiO nanoparticles towards loratadine as a carboxylate-amidic drug compound. Microchem. J. 162 (2021) 105869.
[41] A.J. Bard , L.R. Faulkner , J. Leddy , C.G. Zoski , Electrochemical Methods: Fundamen- tals and Applications, Wiley, New York,
[42] P. Thongnopnua, and C. Poeaknapo, J. Pharm. Biomed. Anal. 37 (2005) 763.
[43] G. Bahrami, and S. Mirzaeei, J. Pharm. Biomed. Anal. 36 (2004) 163.
[44] M. Josefsson, A. L. Zackrisson, and B. Norlander, J. Chromatogr. B 672 (1995) 310.

[45] Martins I, Cristiani FC, Larissa SC, et al. Determination of parabens in shampoo using high performance liquid chromatography with Amperometric detection on a borondopeddiamond electrode. Talanta 85 (2011) 1-7.

[46] V. C. Diculescu, A. Militaru, A. Shah, R. Qureshi, L. Tugulea, and A. M. Oliveira-Brett, J. Electroanal. Chem., 1 (2010) 647.

[47] Asad Ullah, Abdur Rauf, Usman Ali Rana, Rumana Qureshi, Muhammad Naeem Ashiq, Hidayat Hussain, Heinz-Bernhard Kraatz, Amin Badshah, and Afzal Shaha, pH Dependent Electrochemistry of Anthracenediones at a Glassy Carbon Electrode, Journal of The Electrochemical Society, 162 (2015) 157-163.

[48] Prashanth SN, Ramesh KC, Seetharamappa J. Electrochemical oxidation of an immunosuppressant, mycophenolate mofetil, and its assay in pharmaceutical formulations. Int J Electrochem 2011 (2011) 1-7.

[49] D.K. Gosser, Cyclic Voltammetry: Simulation and Analysis of Reaction Mechanisms, VCH, New York, 1993.

[50] H.A. Hendawy , H.M. Elwy , A.M. Fekry , Electrochemical and chemometric determi- nation of dorzolamide and timolol in eye drops using modified multiwall carbon nanotube electrode, Int. J. Pharm. Pharmac. Sci. 9 (2017) 43.

[51] N.P. Shetti , S.J. Malode , D.S. Nayak , S.D. Bukkitgar , G.B. Bagihalli , R.M. Kulkarni , K.R. Reddy , Novel nanoclay-based electrochemical sensor for highly efficient elec- trochemical sensing nimesulide, J. Phys. Chem. Solids 137 (2020) 109210.

[52] A. M. Bond, Modern Polarographic Methods in Analytical Chemistry, Marcel Dekker Inc, USA, 1980.

[53] E. Laviron , General expression of the linear potential sweep voltammogram in the case of diffusionless electrochemical systems, J. Electroanal. Chem. Interfacial Elec- trochem. 101 (1979) 19–28.

[54] A.J. Bard, L.R. Faulkner, Electrochemical Methods: Fundamentals andApplications, Wiley New York,1980.

[55] G. Khaksa, N. Udupa, Rapid and sensitive method for determination of nimesulide in human plasma by high-performance liquid chromatography. J Chromatogr B Biomed Sci Appl 727 (1999) 241–244 .

[56] R.E. Barrientos-Astigarraga, Y.B. Vannuchi, M. Sucupira et al., Quantification of nimesulide in human plasma by high-performance liquid chromatography/tandem mass spectrometry. Application to bioequivalence studies. J Mass Spectrom 36 (2001) 1281–1286.

[57] C. Wang, X. Shao, Q. Liu, Q. Qu, G. Yang and X. Hu, J. Pharm. Biomed. Anal., 42 (2006) 237.

[58] S. Chandran, P. Ravi, P.R. Jadhav, R.N. Saha, A simple, rapid, and validated LC method for the estimation of nimesulide in human serum and its application in bioavailability studies. Anal Lett 41 (2008) 2437–2451.

[59] J. Zhang, X. Tan, D. Zhao, S. Tan, Z. Huang, Y. Mi and Z. Huang, Electrochim. Acta, 55 (2010) 2522.

[60] J. Zhang, X. Tan, D. Zhao, S. Tan, L. Liu, L. Wang and Z. Huang, Chem. Res. Chin. Univ., 27 (2011) 566.

[61] P. F. Pereira, M. C. Marra, A. B. Lima, W. T. P. dos Santos, R. A. A. Munoz and E. M. Richter, Diamond Relat. Mater., 39 (2013) 41.

[62] S. D. Bukkitgar, N. P. Shetti, R. M. Kulkarni, S. B. Halbhavi, M. Wasim, M. Mylar, P. S. Durgi and S. S. Chirmure, J. Electroanal. Chem.,778 (2016) 103.

[63] Mani Govindasamy, Veerappan Mani, Shen-Ming Chen, Highly sensitive determination of non-steroidal anti-inflammatory drug nimesulide using electrochemically reduced graphene oxide nanoribbons, RSC Adv., 7 (2017) 33043–33051.

[64] P.B. Deroco, R.C. Rocha-Filho, O. Fatibello-Filho, A new and simple method for the simultaneous determination of amoxicillin and nimesulide using carbon black within a dihexadecylphosphate film as electrochemical sensor. Talanta 179, (2018) 115–123.

[65] Nagaraj P. Shetti , Shweta J. Malode, Deepti S. Nayak , Shikandar D. Bukkitgar , Gangadhar B. Bagihalli , Raviraj M. Kulkarni , Kakarla Raghava Reddy, Novel nanoclay-based electrochemical sensor for highly efficient electrochemical sensing nimesulide, Journal of Physics and Chemistry of Solids 137 (2020) 109210.

[66] Marcelina Łysoń, Anna Górska, Beata Paczosa-Bator, Robert Piech, Nimesulide Determination on Carbon Black-Nafion Modified Glassy Carbon Electrode by Means of Adsorptive Stripping Voltammetry, Electrocatalysis 12 (2021) 641–649.